

A high precision n-p scattering measurement at 14.9 MeV

N.V. Kornilov^{1,a}, S.M. Grimes¹, T.N. Massey¹, C.E. Brient¹, D.E. Carter¹, J.E. O'Donnell^{1,b}, K.W. Cooper¹, A.D. Carlson², F.B. Bateman², C.R. Heimbach², R.C. Haight³, and N. Boukharouba⁴

¹ Department of Physics and Astronomy, Ohio University, Athens, OH 45701, USA

² National Institute of Standards and Technology, Gaithersburg, MD 20899, USA

³ Los Alamos Neutron Science Center, Los Alamos National Laboratory, Los Alamos, NM 87545, USA

⁴ Department of Physics, University of Guelma, Guelma 24000, Algeria

Abstract. The n-p scattering angular distribution was measured with 14.9 MeV incident neutrons using the traditional time-of-flight technique with neutron-gamma discrimination. The scattering angle varied from 20° to 65° (laboratory system) in 5° incremental steps. The efficiency of the neutron detectors was measured in the energy range 2–9 MeV relative to the ²⁵²Cf-standard, and was calculated using Monte Carlo methods in the 2–14 MeV energy range. Two methods of analysis were applied for experimental and simulated data: a traditional approach with a fixed threshold, and a dynamic threshold approach. The present data agree with the ENDF/B-VII evaluation for the shape of n-p angular distribution within about 1.5%.

1. Introduction

Neutron scattering on hydrogen is one of the most fundamental processes in nuclear physics. The differential cross section for this process is also one of the most important neutron cross section standards. Improving the accuracy of the hydrogen scattering cross section is then important both for a better understanding of the nucleon-nucleon interaction and for improving the knowledge of this quantity as a neutron cross section standard.

A measurement program was initiated as a result of problems that became apparent in evaluations of this cross section. The first measurement [1,2] of this collaboration made by detecting recoil protons was at 10 MeV neutron energy where there is a significant difference in the shape of the angular distribution between the ENDF/B-V and ENDF/B-VI evaluations.

To further improve the quality of the database new measurements were made at 14.9 MeV [3] using the same technique. The results of a first order Legendre polynomial fit are in good agreement in the backward part of the center-of-mass scattering hemisphere with the predictions of the Arndt et al. [4] phase-shift analysis, those of the Nijmegen group [5], and with the ENDF/BVII [6] evaluation.

To examine the n-p scattering cross section at forward angles, one must detect the scattered neutron as the recoil proton has very little energy. Only one experiment [7] has been done at 14.1 MeV at forward angles and it has large uncertainties.

In order to get data at these forward CMS angles in this experiment, the neutrons scatter from a hydrogenous detector (the proton detector) and are detected in a neutron detector.

For the proton-recoil experiments, all angles were measured simultaneously so monitoring of the neutron fluence was not critical. Also the protons are detected with nearly 100% efficiency. In the present experiment monitoring of the neutron fluence must be done accurately since the data are obtained one angle at a time. The efficiency of neutron detectors must be determined with high accuracy.

In this report we describe the experiment, methods of data analysis, estimated uncertainties, final results and conclusions. All uncertainties in this paper are one standard deviation.

2. Experimental method

The experiment was performed at the Ohio University Accelerator Laboratory using the Swinger Spectrometer the beam swinger [8] to change the scattering angle (see Fig. 1). A brief description of the experiment is presented here and a more detailed description will be given later in a full-length report.

Neutrons of 14.9 MeV were generated with a 0.53 MeV deuteron beam on a tritiated titanium target through the T(d,n)⁴He reaction. The neutrons produced at 0-degrees relative to the deuteron beam were incident on the “scatter-detector” (plastic scintillator EJ-200, D = 1.5 cm, H = 4.5 cm, photo multiplier tube (PMT) XP2900) placed about 20 cm from the neutron source. For this detector the threshold of a constant fraction discriminator was fixed at ~60 keV electron energy. This detector produced “stop” signals for the time-of-flight (TOF) measurement.

Three liquid-scintillation neutron detectors (NE213, D = 12.7 cm, H = 5.08 cm, PMT RCA 4522 [9]) were placed in the tunnel at a flight path of 4.108 m from the scatter-detector. These neutron detectors touched each other and provide a “triangle” configuration. The swinger

^a e-mail: kornilov@ohio.edu

^b Deceased

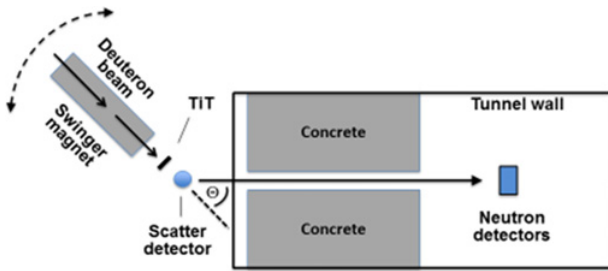


Figure 1. Experimental set up (not to scale).

magnet was rotated about the “scatter-detector” to provide different scattering angles. After splitting the anode signal with a T-splitter, part of the signal was used for timing and the other part for neutron-gamma discrimination.

The threshold for a constant fraction discriminator in the timing channel was adjusted to ~ 30 keV electron energy (half of the ^{241}Am gamma-ray pulse height). These signals were used as “start” signal.

All events (Pulse Height - PH, TOF, and Pulse Shape - PS) were collected in list-mode for each detector with information on how many detectors “fired” for each counting event.

The time-of-flight between the proton detected in the “scatter-detector” and the signal from the NE213 neutron detectors defines the neutron energy and helps to reduce background. Measurements were made from 20° to 65° in 5° steps in the laboratory system. This corresponds to CMS angles from 40° to 130° .

The following additional measurements were made with the neutron detectors looking directly at the source: (1) PH and TOF spectra from $\text{D}(d,n)$ ($E = 7,8,9,10$ MeV) and $\text{T}(d,n)$ ($E = 14.9$ MeV) reactions were used to verify the DYnamic THreshold (DYTH) method [10]; (2) Neutron spectra from the $\text{Al}(d,n)$ reaction ($E_d = 7.44$ MeV) were used to estimate light output for protons; (3) Neutron spectra from a ^{252}Cf (sf) source were used for efficiency estimation for the energy range < 10 MeV. The ^{252}Cf standard data were taken from [11].

3. Analysis of experimental data

3.1. Efficiency of neutron detectors

Two methods were applied for analysis of the same data set: - the traditional approach with fixed bias, and the DYTH method. The fixed threshold allows increased absolute efficiency, and is not sensitive to accurate light output function for protons at high energy. However, the result at high energy is very sensitive to light output for alpha particles, which is practically unknown. The DYTH method requires good knowledge for protons light output, and linearity of the PMT output.

Unfortunately, the neutron detector efficiency cannot be calibrated with the ^{252}Cf (sf) standard over the entire energy range. We compared experimental determination of efficiency with Monte Carlo simulation in the energy range < 9 MeV to validate our models. We then used the model for the energy range 9–13 MeV.

The construction of the ^{252}Cf neutron source and calibration method are described in [12,13]. The fission fragment count rate was about $4 \cdot 10^4 \text{ s}^{-1}$.

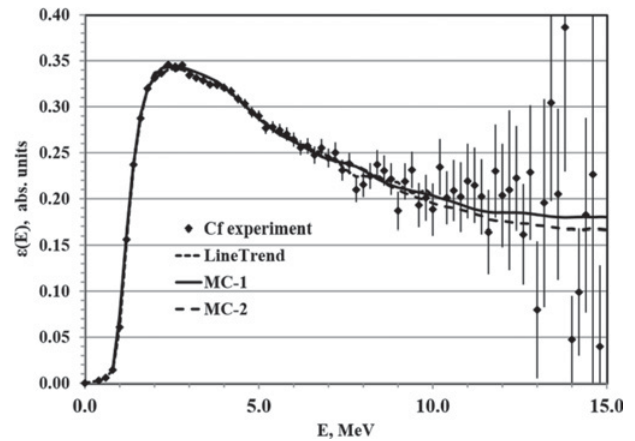


Figure 2. Experimental efficiency and MC simulation for detector 3 (traditional approach). MC-1 – Monte Carlo simulation with original light output determination $L_{\alpha 0}(E)$ for α particles. MC-2 - the same but for $L_{\alpha}(E)=0.5L_{\alpha 0}(E)$. “Line trend” is a smoothed function estimated as a linear function fitted to five experimental points.

3.1.1. Efficiency of the neutron detector for the traditional method and the problem of extrapolation to high energy

The experimental efficiency for detector #3, and the MC results estimated with the traditional approach are shown on Fig. 2. Only statistical uncertainties are given on Figs. 2, 4 for experimental points. The NEFF7 [14] code with incorporation of a new function for the calculation of light output was used in these calculations.

Proton light outputs for each detector were measured with a $\text{Al}(d,n)$ “white neutron spectrum”. Different functions for proton light output were measured for different detectors, which confirmed the conclusion of [13]. The “real” light output for α -particles is poorly known, but this is an important factor for traditional efficiency calculation at high neutron energy.

To understand the scale of this effect, the efficiency for detector 3 was calculated with a light output for α particles included in the NEFF code, and for light output reduced by a factor of 2. The difference at 13 MeV is 6.7% (see Fig. 2).

3.1.2. Light output dependence on proton energy and the saturation problem for DYTH method

The DYTH method is not sensitive to light output for α particles. However, the proton light output is a very important function for successful MC simulation and should be measured for each detector in the whole energy range. The “PMT’s saturation” effect may destroy the results estimated with the DYTH method. Additional measurements of the response functions (RF) and MC simulation were done for monoenergetic neutrons to understand this problem. The experimental and calculated response functions (RF) are shown on Fig. 3.

Both results are in reasonably good agreement for ~ 10 MeV. So for this energy the DYTH method is expected to work reasonably well. At higher energies the situation is more complicated. There is some conflict at 14.9 MeV between experimental data and the MC model used to predict the efficiency of the detector. So this method may

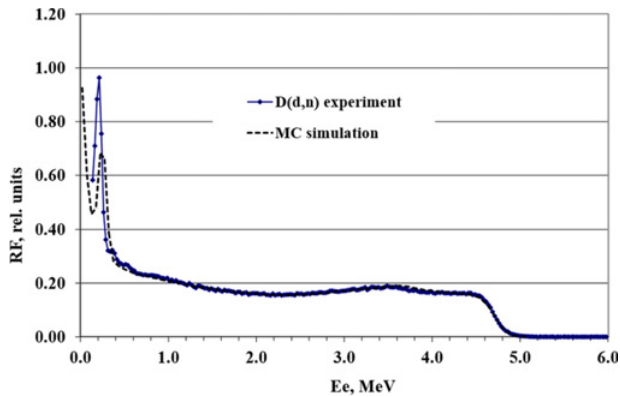


Figure 3. Experimental and calculated RF for incident neutron energy $E=10.27$ MeV.

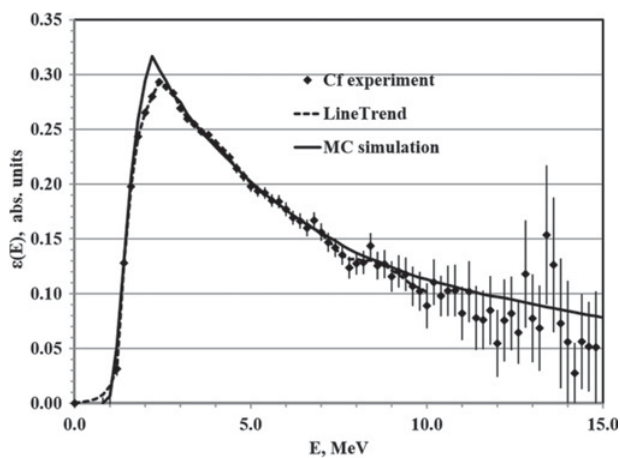


Figure 4. Experimental efficiency (points) and MC simulation (solid line) for detector 3 (DYTH method). Dashed line is the “line trend”.

lead to additional systematic uncertainties. The influence of the saturation effect is rather similar for detectors 2 and 3. Detector #1 had a strong saturation effect even at ~ 10 MeV. Therefore, results measured with detector 1 were not included in the final evaluation.

The efficiency of detector #3 estimated with DYTH is shown in Fig. 3. The Monte Carlo code NEFF7-DYTH based on the code NEFF7 [13] was used for the DYTH analyses. Calculated and experimental efficiencies are in very good agreement in the energy range 2–9 MeV for both methods of data evaluation. Some deviations visible in the range 3–4 MeV (Fig. 2) and ~ 8 MeV (Fig. 4) may be connected with re-scattering of neutrons between detectors which was not included in the MC model, and problems with the neutron angular distribution for scattering from some carbon resonances (see Ref. [15]).

3.2. Interaction of scattered neutrons inside the scatter detector

Another process that may influence the final results is secondary interaction of scattered neutrons in the “scatter-detector”. The “self-absorption” function was calculated applying analytical formulas [15]. The analytical calculations were verified with a MC method (MCNP simulation). The MC method allows us to estimate not only “self-absorption” function but total interaction of scattered

neutrons inside “scatter detector”. Two different calculated runs for each scattering angle were done for normal density ρ (run 1) and 0.001ρ (run 2). The total amount of events in the peak region - N_1 , N_2 were used for calculation of correction factor $\alpha(\theta) = N_1/1000N_2$. Values for $\alpha(\theta)$ are $\alpha(20^\circ) = 0.935$, and $\alpha(65^\circ) = 0.875$. The agreement between MCNP and analytical calculations is about 1%.

3.3. Neutron flux normalization

Normalization of the neutron flux for each angle’s run is a very important factor for accuracy of the final results. Four detectors were applied for this task: - charge integrator, scatter counter with low and high threshold, “stilbene” detector rotating together with the swinger magnet, and a fixed scintillation counter. The ratio of “scatter” detectors with “low” and “high” thresholds was stable with a standard deviation $\sigma = 1.1\%$. For the ratio of the “stilbene”, and “scatter” detectors $\sigma = 4\%$. For the charge integrator and fixed scintillator standard deviations were $>10\%$. To reduce the uncertainties we choose only “scatter”, and “rotating stilbene” detectors were used for normalization.

4. Systematic uncertainties and results

Several factors contribute to uncertainties of the experimental results. We do not have any algorithm to select the energy range for “peak” integration and calculation of the background function. In our evaluation, the simple “line” function for background was applied. The limits of the integration interval were selected empirically.

There is a “low energy tail” which is visible at small scattering angles (high energy neutrons) in the scattering spectrum. There was also a broad distribution in the energy range about 5 MeV visible in experimental spectra. These added about 5% to the absolute uncertainty, most of which canceled when considering only the cross section shape.

The angular results measured with two detectors and two methods of data evaluation are in reasonable agreement. Each of the four data sets was normalized separately with its own overall normalization factor to the ENDF/B-VII [6] evaluation to minimize the deviation from the evaluation. The analysis of these data showed that, within the statistical uncertainties, all the data are in agreement.

We applied two methods for each detector. All factors mentioned above are different for each detector and method. Thus we may assume that we have *four mainly independent results for each angle*. Hence, the final data and their uncertainties may be found as the average values and standard deviation (STD) combined with systematic uncertainties.

Two systematic uncertainties were included in total uncertainties. Those for lower energies”: - uncertainties in ^{252}Cf as a standard 1.2% (3 MeV) – 2.5% (10 MeV), - those for higher energies, uncertainties for the efficiency calculation 2.5% (11 MeV), and 4% (13 MeV), These final results are shown in Table 1.

Our final n-p scattering cross sections and uncertainties are shown on Fig. 5 together with evaluated data. The

Table 1. Final results.

| θ_{LS} ($^{\circ}$) | $\cos(\Theta)$ in CMS | E MeV | $\langle\sigma_{np}\rangle$ mb/sr | Std % | Syst unc. % | total unc. % | Ratio to B-VII |
|---------------------------------|-----------------------------|----------|--------------------------------------|----------|-------------------|--------------------|----------------------|
| 20 | 0.766 | 13.16 | 49.18 | 2.2 | 4.0 | 4.5 | 0.985 |
| 25 | 0.643 | 12.24 | 49.25 | 2.4 | 3.0 | 3.8 | 0.983 |
| 30 | 0.500 | 11.18 | 50.70 | 2.1 | 2.5 | 3.2 | 1.007 |
| 35 | 0.342 | 10.00 | 50.48 | 1.7 | 2.5 | 3.0 | 0.997 |
| 40 | 0.174 | 8.74 | 51.75 | 2.8 | 2.1 | 3.5 | 1.016 |
| 45 | 0.000 | 7.45 | 52.13 | 0.4 | 1.8 | 1.8 | 1.017 |
| 50 | -0.174 | 6.16 | 51.97 | 2.0 | 1.5 | 2.5 | 1.007 |
| 55 | -0.342 | 4.90 | 52.88 | 1.5 | 1.4 | 2.1 | 1.017 |
| 65 | -0.643 | 2.66 | 51.89 | 2.0 | 1.2 | 2.3 | 0.980 |

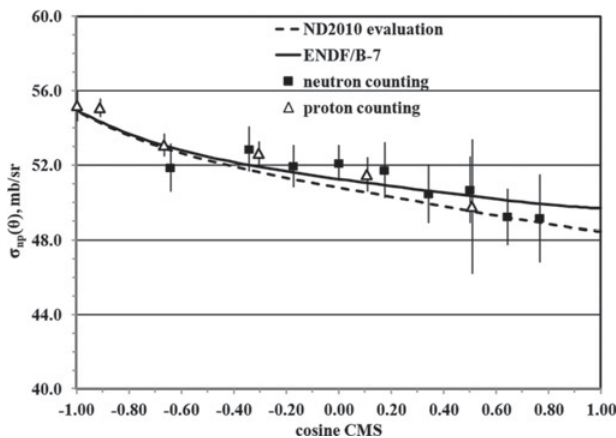


Figure 5. Average experimental data and total uncertainties as are shown in Table 1. Evaluation given by dashed line was taken from [17].

experimental results measured with protons counting in a previous experiment [3] are plotted also.

We should highlight the very good agreement (2–3%) between experimental results measured with different techniques. The data spread is inside the estimated uncertainties. This gives us an additional argument, that experimental procedure and data treatment were done correctly. The total uncertainties are estimated in proper way also.

The average ratio to ENDF/B-VII and its standard deviation are 1.001 ± 0.015 . Due to the normalization procedure describe above, this perfect agreement of the average value confirms the normalization procedure only. But the data spread 1.5% is the realistic estimation of uncertainties for the shape experiment. Of course it is true if reference evaluation is correct.

5. Conclusions

- The angular distribution of (n,p) scattering cross section was measured by neutron counting for incident neutron energy 14.9 MeV;
- Our experimental results agree with the ENDF/B-VII shape evaluation within 1.5%;
- In this investigation we reached the realistic limit of uncertainties, for the type of experiment we performed.

This work was performed under the auspices of the U.S. DOE: agreements DE-AC5206NA25396 (LANL), DE-SC0011527 (NIST), and grants DE-FG02-88ER0387, DE-FG07-07ID14887 (OU). Thanks to staff and operators at the Ohio University Accelerator Laboratory for their efforts.

References

- [1] N. Boukharouba, et al., Phys. Rev. C **65**, 014004 (2002)
- [2] N. Boukharouba, et al., Phys. Rev. C **82**, 039901(E) (2010)
- [3] N. Boukharouba, et al., Phys. Rev. C **82**, 014001 (2010)
- [4] R.A. Arndt, I.I. Strakovsky, and R.L. Workman, Phys. Rev. C **50**, 2731 (1994)
- [5] J.J. de Swart, et al., Few-Body Syst., Suppl. **8**, 438 (1995)
- [6] A.D. Carlson, et al., Nucl. Data Sheets **110**, 3215 (2009)
- [7] A. Suhami, and R. Fox, Phys. Lett. B **24**, 173 (1967)
- [8] R.W. Finlay, et al., Nucl. Instr. and Meth. **198**, 197 (1982)
- [9] G. Randers-Pehrson, et al., Nucl. Instr. and Meth. **215**, 433–436 (1983)
- [10] N.V. Kornilov, S.M. Grimes, and T.N. Massey, report for NEMEA-7/CIELO workshop 5–8 Nov. 2013, NEA/NSC/DOC(2014)13, pp. 221–227
- [11] <https://www-nds.iaea.org/standards/>
- [12] N.V. Kornilov, et al., Scientific Report 2005, EUR 22239 EN (2006), p. 45
- [13] N.V. Kornilov, et al., Nucl. Instr. & Meth., A **599**, 226 (2009)
- [14] G. Dietze, and H. Klein, Nucl. Instr. & Methods **193**, 549 (1982)
- [15] N.V. Kornilov, IAEA report INDC(USA)-108, 2015
- [16] N.V. Kornilov. Fission neutrons, experiment, evaluation, modeling and open problems, ISBN: 978-3-319-07132-9, Springer, 2015
- [17] N.V. Kornilov, T.N. Massey, and S.M. Grimes, J. Korean Phy. Soc. **59**, 1404 (2011)